Diyala Journal of Engineering Sciences

Journal homepage: https://djes.info/index.php/djes

ISSN: 1999-8716 (Print); 2616-6909 (Online)

# Improving the AVR Performance of Iraqi Hamrin Hydro Station Using PID Controller Optimized by GWO and WOA

Rasha Yasen Abed*, Zeina K. Gurgi

Department of Electrical Power and Machines, College of Engineering, University of Diyala.

**ARTICLE INFO**

**Article history:**
Received 18/01/2025.
Revised 22/09/2025.
Accepted 24/11/2025.
Available online 15/06/2026.

**Keywords:**
Automatic Voltage Regulator
Gray wolf optimization
Whale optimization method
Integral time absolute error
Integral time square error

**ABSTRACT**

*Power grid reliability and voltage stability are important factors for the stable operation of hydropower plants. Automatic Voltage Regulators (AVRs) contribute to maintaining stability by controlling generator excitation and terminal voltage. Achieving the best possible AVR performance is considered an important challenge. This study presents a comparison of two optimization algorithms—the Grey Wolf (GWO) algorithm and the Whale (WOA) algorithm—for selecting the optimal proportional-integral-derivative (PID) controller parameters in an AVR system. The optimization process uses two performance index equations, the integral of the time absolute error (ITAE) and the integral of the time square error (ITSE). The performance evaluation and Simulations were conducted using MATLAB/Simulink. The results showed that the ITSE method based on the Whale Optimization Algorithm (WOA) achieves a faster response, while the Gray Wolf Optimization (GWO-ITSE) algorithm was superior in stability performance. By using GWO-ITSE, the maximum deviation was decreased from 1.58 p.u. to 1.03 p.u. with 34.8% approximate enhancement. Moreover, the settling time (sec) was reduced from 18 seconds to 7.5 seconds with 58.3% approximate improvement. As a result, the GWO-ITSE proposed more stability in these hydropower plants and can be more suitable for similar applications. The obtained results further highlight the improved AVR performance using optimized PID parameters*

## 1. INTRODUCTION

An automatic voltage regulator (AVR) is essential for power system companies to adjust and control the voltage of a synchronous generator. It helps maintain the output voltage within specified limits despite load changes or other factors that may affect it. A voltage regulator helps protect connected devices from faults caused by voltage fluctuations. An automatic type is commonly used in power plants, distribution systems, and industrial applications to provide a stable and reliable power supply [1].

Variations in generator power output are primarily due to sudden load fluctuations, which significantly impact system stability. To mitigate these fluctuations, PID (proportional-integral-differential) controllers are widely used in modern control systems. Using advanced control algorithms and sensors to monitor the system, adjust generator output, and ensure a fast and consistent response. By incorporating a feedback mechanism and a compensator, a PID controller contributes to highly efficient power delivery and system performance that adapts to changing load requirements and conditions.

This study analyzes the impact of optimizing an FOPID controller for AVR systems using a modified smoothed function algorithm. The analysis focuses on key performance indicators such as overshoot, rise time, settling time, steady-state error, and computational load measured by the number of function evaluations. Robustness, disturbance rejection, and parameter variability are examined using the IAE, ISE, ITAE, and ITSE metrics [2].

Finding the best setting for a PID controller gain parameter can be difficult. This is so that the proper values of these parameters can vary depending on the operating conditions and the dynamics of the controlled system, which might be complicated and nonlinear. PID

*Corresponding author's E-mail: rashaabed876@gmail.com
DOI: 10.24237/djes.2026.19207

controllers can be tuned using a variety of techniques. Firstly, trial-and-error can be useful in certain situations, but it can also be time-consuming and inefficient. Alternatively, to address these limitations, more methods like the Ziegler-Nichols technique have been developed. Involves adjusting the controller settings until sustained oscillations occur, after which the parameters are fine-tuned to stabilize the system [3]. However, these two approaches produce an unfavorable failure to determine the optimal PID settings, as well as overshoots, slow response time, steady-state error, and long-term oscillations in the system.

Contrarily, artificial intelligence methods like fuzzy and neural networks are used to identify the optimal PID solution as detailed in [4] and [5]. Both artificial neural networks and fuzzy logic systems have unique difficulties and complications. Artificial neural networks require a lot of data and computer power to train, which might take a long time. On the other hand, the successful development of fuzzy membership functions for fuzzy logic systems necessitates data analysis, model tuning, and designer knowledge, which can be a subjective process [6, 7].

Evolutionary-based heuristic optimization algorithms use techniques inspired by naturalism to investigate the best values of a set of parameters. For example, when setting the parameters of the PID controller in the system of automatic voltage regulation, the algorithm would start by randomly assigning values to the controller parameters. The performance of the automatic voltage regulation system with these parameter values would then be evaluated based on a predefined fitness function that quantifies the performance of the system. This method is recurrent while the best solution is found. Advantages of these algorithms include their ability to handle complex nonlinear problems, their ability to search the entire solution space, and their ability to find near-optimal solutions. Instead, they employ the aforementioned conventional tuning techniques, which perform poorly and are ineffective when used in varied operating environments.

Modern tuning techniques based on heuristic optimization, such as Teaching–Learning Based Algorithm (TLBA). Therefore, Heuristic optimization offers an effective solution more than traditional tuning methods, which may struggle to cope with system complexity [1],the optimization method of Gradient-Based (GBO) Algorithm[8], organism search of symbiotic optimization algorithm , optimization of Particle swarm and algorithm of Whale optimization [9], optimization of particle swarm and bee colony algorithms[10], optimization algorithm of teaching–learning-based [11], Taguchi combined of genetic algorithm [12], optimization algorithm of anarchic society [13], optimization algorithm of bacterial foraging (BFOA)[14], Chaotic differential evolution algorithm (CDEA) [15], stochastic fractal search algorithm(SFSA) [16], sine cosine algorithm (SCA)[17], Algorithm of Salp Swarm[18], search of hybrid harmony and optimization algorithms of dwarf mongoose [19], Non Monopolize Search [20],optimization of cuckoo search (CSA) [21], Ant Lion Optimizer Algorithm (ALOA) [22], Tree Seed Algorithm ( TSA), kidney-inspired algorithm (KA), have been applied to all common optimization algorithms used for tuning PID controllers. Choosing the right algorithm for a given task is crucial. The algorithms mentioned above aim to find the optimal values that cause the best performance of an automatic voltage regulation system.

The objectives of the studies mentioned above are multiple and can be summarized as reducing several things, including steady-state error, maximum overshoot, the time of rise, settling, and peak. To evaluate the performance of the control unit, several indicators are often used: ITAE, ITSE, IAE, and ISE [3], [23-26].

In robotics and automated systems where response time is of utmost importance, we use the ITAE function, which is based on maintaining the accuracy of the system and reducing the response time. When stability is more important than response time, we use the ITSE function. The IAE function is used when the difference between the desired values and the actual output is insignificant. The ISE function is used when the primary focus is on suppressing sudden spikes in the system's response. In general, the choice of objective function for an AVR PID depends on the type of system and its specific constraints.

When using PID controllers in nonlinear environments, they face several challenges. These challenges have led researchers to explore and develop more flexible and effective control techniques to improve the performance of non-PID AVR systems. These techniques include: For systems in nonlinear and uncertain environments that do not require an accurate mathematical model, the fuzzy logic controller (FLC) is the first choice for researchers. [27,28] Sliding mode control (SMC) is often suitable for handling sudden changes in the system due to its responsiveness and resistance to disturbances and distortions [29,30]. Using Neural Network Controller (NNC) in AVR can provide treatment for uncertain system behavior and can be highly resilient to system changes, especially when it is difficult to model mathematically [31,32]. The Linear Quadratic Regulator (LQR) offers precise stability performance; however, its challenges lie in its reliance on complex mathematical models [33,34]. Adaptive control is known for its capability to automatically regulate its parameters in response to modifications in system dynamics. For this reason, it is an exemplary choice for controlling unstable or those that are difficult to control precisely mathematically [35]. Although many optimization algorithms have been used to find PID parameters in AVR systems, no research has

specifically addressed the AVR system at the Hamrin hydro power station.

In this paper, two optimization methods (GWO and WOA) were used to obtain the optimal PID parameters. The PID controller was used in the proposed model of the Hamrin Hydro power station to improve the performance of the AVR. Both methods proposed promising results; however, the GWO was superior to WOA in the simulation results. Hence, the proposed model can be utilized by the system operator to enhance the voltage stability performance at the Hamrin hydro power station.

## 2. MODELING OF THE PID CONTROLLER

The PID controller is considered one of the most widely used in industrial applications. This system is characterized by its simplicity, efficiency, and robustness, and is suitable for various industrial control systems. It can be represented mathematically using equations in the Laplace domain.

$$G(s) = \frac{U(s)}{E(s)} = k_p + \frac{k_i}{s} + k_d * s \quad (1)$$

the control signal equation can be written in terms of the time domain:

$$u(t) = \left(k_p e(t)\right) + (k_i \int_0^t e(t)dt) + (k_d \frac{de(t)}{dt} \quad (2)$$

$k_p$ proportional gain, $k_i$ Integral gain, and $k_d$ derivative gain. This study examines the effects of two objective functions on parameter optimization. The first objective, ITAE, reduces the effectiveness of initial errors in the final performance evaluation by assigning a time weight to errors, thereby enhancing system performance. A second objective, the ITSE Index, represents multiplying the integral time by the squared error. Have the following definitions:

$$ITAE = \int_0^t \mathrm{t} \,.\, |e|\, dt \quad (3)$$

$$ITSE = \int_0^t t.e^2 \; dt \quad (4)$$

- t = Time
- e = error signal between the reference input and the system output

## 3. MODELLING OF AUTOMATIC VOLTAGE REGULATION SYSTEM.

Hamrin Hydroelectric Station is one of the Iraqi stations. This station generates electrical energy through the dam on the Diyala River. And the water energy is converted into mechanical energy through hydraulic turbines and then into electrical energy using electric generators. Based on information provided by the Iraqi Ministry of Electricity, specifically from the control centre. Generally, an automatic voltage regulator consists of three main parts, the first of which is a synchronous generator, which describes its voltage performance and its contents

- Synchronous -reactance: $X_d$=1.0 p.u
- Transient- reactance: $X'_d$=0.7 p.u
- Sub transient- reactance: $X''_d$=0.2158 p.u
- Open-circuit transient constant of time: $X'_{do}$=1.065 second

Calculate the gain based on dividing the synchronous reactance by the difference between the transient reactance and sub-transient reactance.

$$K_g = \frac{X_d}{(X'_d - X''_d)} \quad (5)$$

$$K_g = \frac{1.0}{(0.70-0.2158)} = 0.4842 \quad (6)$$

- Calculation of time constant:

$$T_g = T'_{do} \times \left(\frac{(X_d - X'_d)}{X'_d}\right) \quad (7)$$

$$T_g = 1.065 \times \left(\frac{(0.7-0.3)}{0.7}\right) = 2.486 \text{ sec} \quad (8)$$

- The transfer function for the generator is:

$$G(s) = \frac{K_g}{(sT_g+1)} \quad (9)$$

$$G(s) = \frac{0.4842}{2.4865s+1} \quad (10)$$

This form presents a simplified and practical conception of voltage dynamics generators, particularly for use in linear system control analysis and AVR design. The DC exciter is used in the standard ESDC1A format, which models an excitation system of classical direct current. The model inputs were obtained from operational data supplied by the Iraqi Ministry of Electricity of the Hamrin Hydropower Station. The excitation system is depicted by the structure of the transfer function:

$$G_{exc}(s) = \frac{K_e}{sT_e+1} \quad (11)$$

- The exciter Transfer function $G_{exc}(s)$
- The exciter Gain $K_e$ =1
- Time constant of the exciter $T_e s$=0.46

Under specific conditions, predominantly when the exciter proceeds like a pure integrator, it can be simplified and written as:

$$\frac{1}{sT_e} = \frac{1}{0.46\, s} \quad (12)$$

The amplifier's attitude can be illustrated by the following transfer function equation:

$$G_{amp}(s) = \frac{K_A}{sT_A+1} \quad (13)$$

Where:

- $G_{amp}(s)$: The amplifier Transfer function
- $K_A$ : Gain amplifier =50
- $T_A s$ : Time constant =0.06 seconds

The following transfer function equation specifies the sensor representation:

$$G_{sensor}(s) = \frac{sK_s}{sT_s+1} \quad (14)$$

$$G_{sensor}(s) = \frac{0.1s}{s+1} \quad (15)$$

- Gain sensor $K_s$ = 0.01
- Time constant $T_s$ =1 second

Table 1 presents the electrical and control parameters. MATLAB Simulink Model of an AVR System is Illustrated in Figure 1.

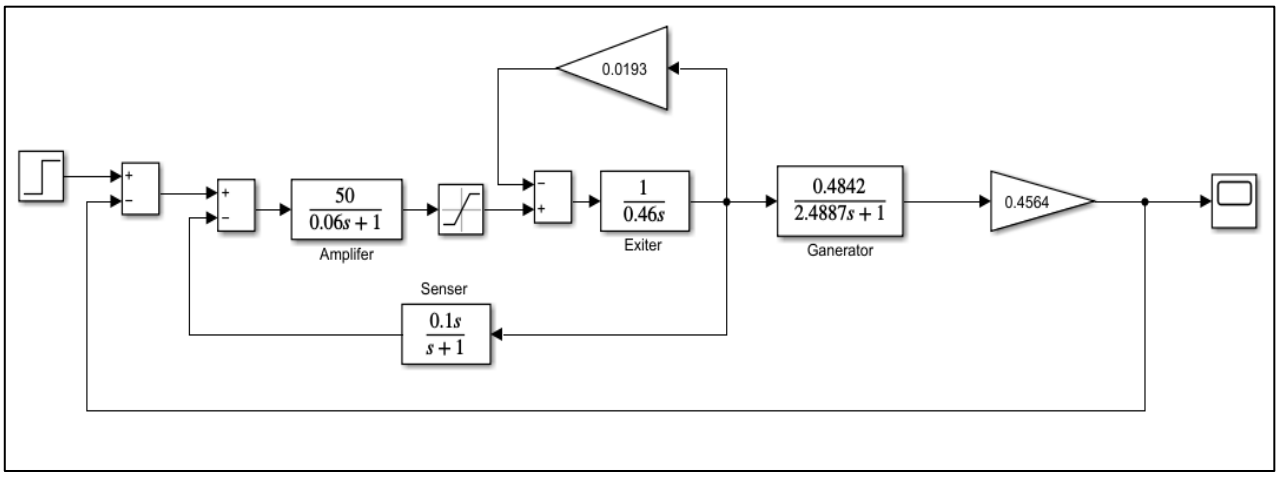


**Figure 1**. MATLAB/Simulink Model of an AVR System for a Generator.

**Table 1**. Parameters of the Synchronous Generator and Excitation System Model

| Component | Parameter | Symbol | Value |
|---|---|---|---|
| **Synchronous Generator** | Synchronous reactance | Xd | 1.0 p.u. |
| | Transient reactance | Xd′ | 0.7 p.u. |
| | Sub-transient reactance | Xd″ | 0.215 p.u. |
| | Open-circuit transient time constant | Tdo′ | 1.065 s |
| | Generator gain | Kg | 0.4842 |
| | Generator time constant | Tg | 2.4865 s |
| **Exciter** | Exciter gain | Ke | 1 |
| | Exciter time constant | Tes | 0.46 s |
| **Amplifier** | Amplifier gain | KA | 50 |
| | Amplifier time constant | TA | 0.06 s |
| **Sensor** | Sensor gain | Ks | 0.01 |
| | Sensor time constant | Ts | 1.0 s |

## 4. OPTIMIZATION TECHNIQUES

To optimize and tune the AVR controller parameters, we use mathematical optimization algorithms to achieve a balance between accuracy and speed. Our selection of optimization methods must take into account simple computational requirements and make them suitable for real-time applications .

The Grey Wolf algorithm can exhaustively explore the search space in the early stages and then gradually transition to the second stage, the exploitation stage. This increases the chance of finding a globally optimal solution and reduces the probability of finding local solutions.

The WOA algorithm provides greater flexibility in finding optimal solutions and achieves a balance between exploitation and exploration during its implementation. Although other algorithms exist, such as the Lion Optimization Algorithm (LOA), Harris Hawks Optimization (HHO), and Chimp Optimization Algorithm (ChOA) and others, these algorithms always require long computational time and more sensitive tuning parameters to achieve the same level of accuracy, which may not be suitable when dealing with dynamic models that require frequent and rapid testing, such as AVR systems. Furthermore, some of these algorithms may suffer from performance degradation when the problem dimension increases or when multiple constraints are present.

*4.1 Gray Wolf Algorithm (GWA)*

The Gray Wolf is part of the canine family. They are known as apex predators and have a strict and dominant social hierarchy.

Level (1)—The wolf that dominates the group is the Alpha wolf. It determines the responsibility for making decisions in the pack. The pack must follow and obey his orders.

Level (2)—The Beta wolf occupies the second position in the hierarchy of Gray wolves. He participates in pack activities or helps the Alpha in making decisions

Level (3)—Delta wolves come in third place after Alpha and Beta in the pack hierarchy. They play important roles in maintaining the stability and organization of the pack.

Level (4)—Omega is considered the lowest-ranking wolf in the hierarchy. it's often displaying submissive behaviour to ensure that it does not pose a danger or threat to any pack member.

According to Muro et al. [36], the group hunting of Gray wolves is carried out in stages: the first stage is identifying the prey, following it, and approaching it.

The second stage is surrounding the prey after it stops moving. The third stage is attacking the targeted prey from all sides.

*4.1.1 Algorithm and mathematical model*

This section discusses the mathematical model of a search, surrounding, and assaulting hierarchy. In social hierarchy, alpha is referred to as the fittest, resulting in this context, while beta is the second solution, and delta is the third solution. All remaining will refer to omega [38]. Equations (5) and (6) describe the mathematical method of encircling the prey.

$$\overrightarrow{D} = \left|\left(\overrightarrow{C} \,.\, \overrightarrow{X_p}(t)\right) - \vec{X}(t)\right| \quad (16)$$

$$\vec{X}(t+1) = \left(\overrightarrow{X_p}(t)\right) - \left(\overrightarrow{A} \,.\, \vec{D}\right) \quad (17)$$

$\overrightarrow{D}$ represents the distance vector between the location of the gray wolf $\vec{X}(t)$ and the location of the prey $\overrightarrow{X_p}(t)$ after modifying it by the coefficient $\vec{C}$ . $\vec{X}(t+1)$ represents an updated equation for the location of the gray wolf. The vectors $(\vec{A})$ and$(\vec{C})$ are computed in the following way:

$$\overrightarrow{A} = 2\overrightarrow{a}.\overrightarrow{r_1} - \overrightarrow{a} \quad (18)$$

$$\overrightarrow{C} = 2\,.\overrightarrow{r_2} \quad (19)$$

$\overrightarrow{\boldsymbol{A}}$ as a random vector within the range [-a, a], with a decreasing from 2 to 0 over iterations. When random values fall within [-1, 1], the search agent's location is updated each iteration, and the new position is likely closer to the prey. The search agent's location in each iteration, and the new location can be the nearest to the prey.

To perform a mathematical simulation of the hunting, we will need to: based on the behavior of grey wolves, we hypothesize that the alpha wolf is the best candidate solution, and the beta wolf and the delta wolf have preferable information concerning the possible locations of prey animals. To find the optimal solutions, we will select the three best solutions: Alpha, Beta, and Delta. After that, we will instruct other agents, including Omega, to adjust their positions based on those solutions. The following equations are proposed for consideration.

$$\begin{aligned}
\overrightarrow{D_{\alpha}} &= \left|\left(\overrightarrow{C_1}.\,\overrightarrow{X_{\alpha}}\right) - \overrightarrow{X}\right| \\
\overrightarrow{D_{\beta}} &= \left|\left(\overrightarrow{C_2}.\,\overrightarrow{X_{\beta}}\right) - \overrightarrow{X}\right| \\
\overrightarrow{D_{\delta}} &= \left|\left(\overrightarrow{C_1}.\,\overrightarrow{X_{\delta}}\right) - \overrightarrow{X}\right|
\end{aligned} \quad (20)$$

$$\begin{aligned}
\overrightarrow{X_1} &= \overrightarrow{X_{\alpha}} - \left(\overrightarrow{A_1}.\left(\overrightarrow{D_{\alpha}}\right)\right) \\
\overrightarrow{X_2} &= \overrightarrow{X_{\beta}} - \left(\overrightarrow{A_2}.\left(\overrightarrow{D_{\beta}}\right)\right) \\
\overrightarrow{X_3} &= \overrightarrow{X_{\delta}} - \left(\overrightarrow{A_3}.\left(\overrightarrow{D_{\delta}}\right)\right)
\end{aligned} \quad (21)$$

$$\vec{X}(t+1) = \frac{\left(\overrightarrow{X_1}+\overrightarrow{X_2}+\overrightarrow{X_3}\right)}{3} \quad (22)$$

Depending on the locations of the three solutions, Alpha, Beta, and Delta, we will assume that these three points form a circle and the location of the prey is inside this circle. As for the rest of the agents, including Gama, they will update their locations to be inside this circle.[36].

To mathematically model the wolves' approach to the prey, we reduce the value of $(\overrightarrow{a})$ . It should be noted that the area of inconstancy of $(\overrightarrow{A})$ is also reduced by $(\overrightarrow{a})$ .

At the beginning of the algorithm, random locations are chosen for the gray wolves in the search space. The wolves compete with each other to reach the optimal solution. The alpha, beta, and delta wolves update their locations through iterative mathematical equations to approach the prey. With each iteration, the distance between the wolf and the prey will decrease [36-38]. The flowchart illustrating the GWO process is shown in Figure 2.

*4.1.2 Gray Wolf Optimization Algorithm for PID Controller Tuning*

1- The population size is specified as 30, and the number of iterations is 50
2- Starting randomly PID controller parameters (Kp, Ki, Kd). between limits Kp ∈ [0,3], Ki ∈ [0, 3], Kd ∈ [0, 3]. These limits rely on the system's prerequisites.
3- Select the Performance Index :We use ITAE in equation (3), and ITSE in equation (4). The objective is to minimize ITAE or minimize ITSE.
4- Fitness Evaluation: To calculate the best solution, each wolf in the entire population represents a potential solution with a set of different PID values. We calculate the values of the two performance indicators used in the proposed method (ITAE or ITSE).
5- Position Update: In this part, the GWO algorithm updates the PID values for each solution obtained. After the update process is performed based on α, β, and δ, the new location for each solution is calculated by taking the average of the resulting locations, ensuring that the results gradually converge toward the optimal location.
6- Optimal Solution Extraction :In the final stage, the stopping condition is checked when the maximum number of iterations is reached. At stopping, the PID coefficients of the solution α are the optimal values that achieve the lowest possible value of the index (ITSE or ITAE). This results in the final optimized values.

*4.2 Whale Optimization Algorithm (WOA)*

The Scientists Mirjilili and Lewis proposed an approach to evaluating the complex hunting behaviours of humpback whales while hunting their small fish prey, which includes three stages [39,40].

*4.2.1 Prey Encirclement Behavior*

Whales locate prey and begin encirclement. The Whale Optimization Algorithm (WOA) assumes the ideal route is the optimal solution or nearby, and the other

whales readjust their positions toward the best path discovered. The procedure is delineated as follows:

$$\vec{D} = \left|\vec{C} \cdot \overrightarrow{X^*} - \vec{X}(t)\right| \quad (23)$$

$$\vec{X}(t+1) = \overrightarrow{X^*}(t) - \vec{A} \cdot \vec{D} \quad (24)$$

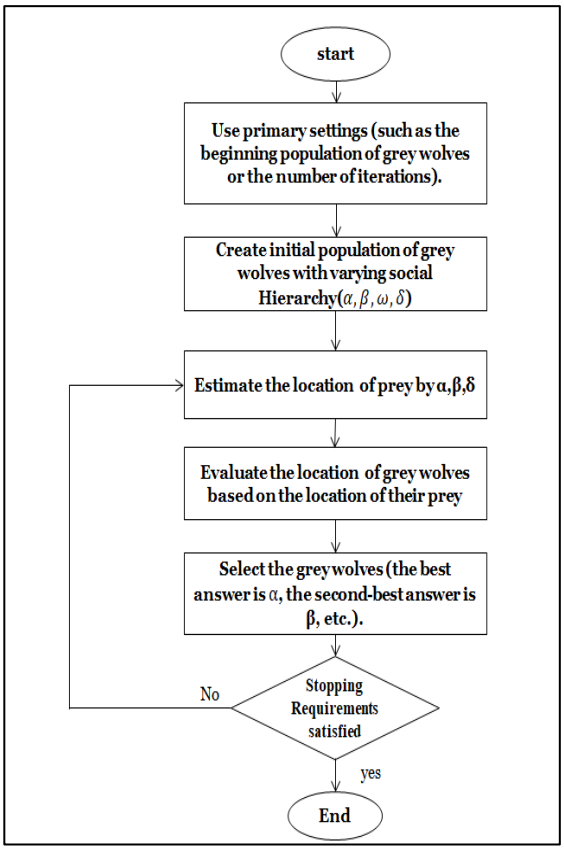


**Figure 2.** Flow Chart of GWO Algorithm.

The mathematical equation used to determine the vectors $\vec{A}$ and $\vec{C}$ are mentioned in the equation below

$$\vec{A} = 2\,\vec{a} \cdot \vec{r} - \vec{a} \quad (25)$$

$$\vec{C} = 2 \cdot \vec{r} \quad (26)$$

Vector $\overrightarrow{r}$ is a randomly selected value within [0, 1]. The variable $\overrightarrow{a}$ takes values from 2 to 0 and undergoes a linear reduction during the iterations. Different locations close to the optimal position may be attained by considering vectors $\vec{A}$ and $\vec{C}$. Consequently, Modified Equation 4 can utilize an approximation factor to bring the result closer to the optimal solution, thereby reducing the whales' locations around the prey.

*4.2.2 The Bubble-net Hunting Process*

Whales use two hunting strategies. The first strategy is to use the contraction method to encircle the prey by updating $\overrightarrow{A}$, discovering all nearby locations along the optimal movement path, and modifying the vector $\overrightarrow{a}$. WOA uses helix technology to update locations and calculate the discrepancy between the prey and other whales.

$$\vec{X}(t+1) = \overrightarrow{D'} \cdot e^{bl} \cdot \cos\left(2\pi l + \overrightarrow{X^*}(t)\right) \quad (27)$$

In this context, $\overrightarrow{D'}$ represents the distance between the nearest whale and the prey. When whales search for their prey, they follow a path resembling a logarithmic spiral, constantly expanding and becoming farther from the center, which helps them discover new areas. This is represented by the equation with the variable $b$ while $l$ represents a randomly selected value within [-1, 1]. update method for the whales' locations (shrinkage or spiral) occurs with a 50% chance for each search iteration, as illustrated in equation 24

$$\begin{cases} (\overrightarrow{X^*}(t) - (\vec{A}.\vec{D})) \text{ if P} < 0.5 \\ \vec{X}(t+1) = \overrightarrow{D'}.e^{bl}.Cos\left(2\pi l + \overrightarrow{X^*}(t)\right) \text{ if P} \geq 0.5 \end{cases} \quad (28)$$

The third stage of prey search involves a distinct approach by whales. In this predation phase, a designated agent conducts a random search using the coefficient vector described in the algorithm. The range of values for the variable $\vec{A}$ is [-1, 1]. To discover more prey, various whales hunt at $\vec{a}$ considerable distance from the reference whale. The current updating method involves selecting a new whale at random, as represented in the equation below.

$$\vec{D} = \left|\vec{C}.\overrightarrow{X_r} - \vec{X}(t)\right| \quad (29)$$

$$\vec{X}(t+1) = \overrightarrow{X_r} - \vec{A}.\vec{D} \quad (30)$$

The variable $Xr$ represents a random whale chosen from among the whales during the exploration period. This step helps expand the search period [41-43].

*4.2.3 Whale Optimization Algorithm (WOA) for PID Tuning in AVR*

1. The population size is specified as 30, and the number of iterations is 50
2. Initialize PID controller parameters arbitrarily. The starting PID controller parameters are generated within the following limits: Kp ∈ [0, 3], Ki ∈ [0, 3], and Kd ∈ [0, 3]. These limits rely on the system's prerequisites. These limits rely on the system's prerequisites.
3. Select the Performance Index: We use ITAE or ITSE as the performance criterion. The objective is to minimize the selected index.
4. Fitness Evaluation: Each whale in the population represents a candidate solution with a unique set of PID values. The AVR system model is simulated with these values, and the selected performance index (ITAE or ITSE) is computed. After evaluation, all whales are ranked from best to worst, with the best whale representing the optimal solution at this stage.
5. Update Positions: The positions of whales (PID coefficients) are updated according to the whale hunting strategies described in the WOA:
   - Encircling the prey: update the position around the best solution using equations (23) to (26).
   - Bubble-net spiral update: move in a logarithmic spiral path around the best solution by using

equation (27), or spiral motion by using equation (28).

- Exploration phase: the algorithm randomly chooses another solution and updates positions by using equations (29) and (30).

6. Optimal Solution Extraction: When the maximum number of iterations is reached and termination occurs, the PID parameters of the best solution and the minimum value of ITSE or ITAE.

This process results in the final optimized PID controller values for the AVR system. A diagram of the WOA algorithm sequence is shown in Figure 3.

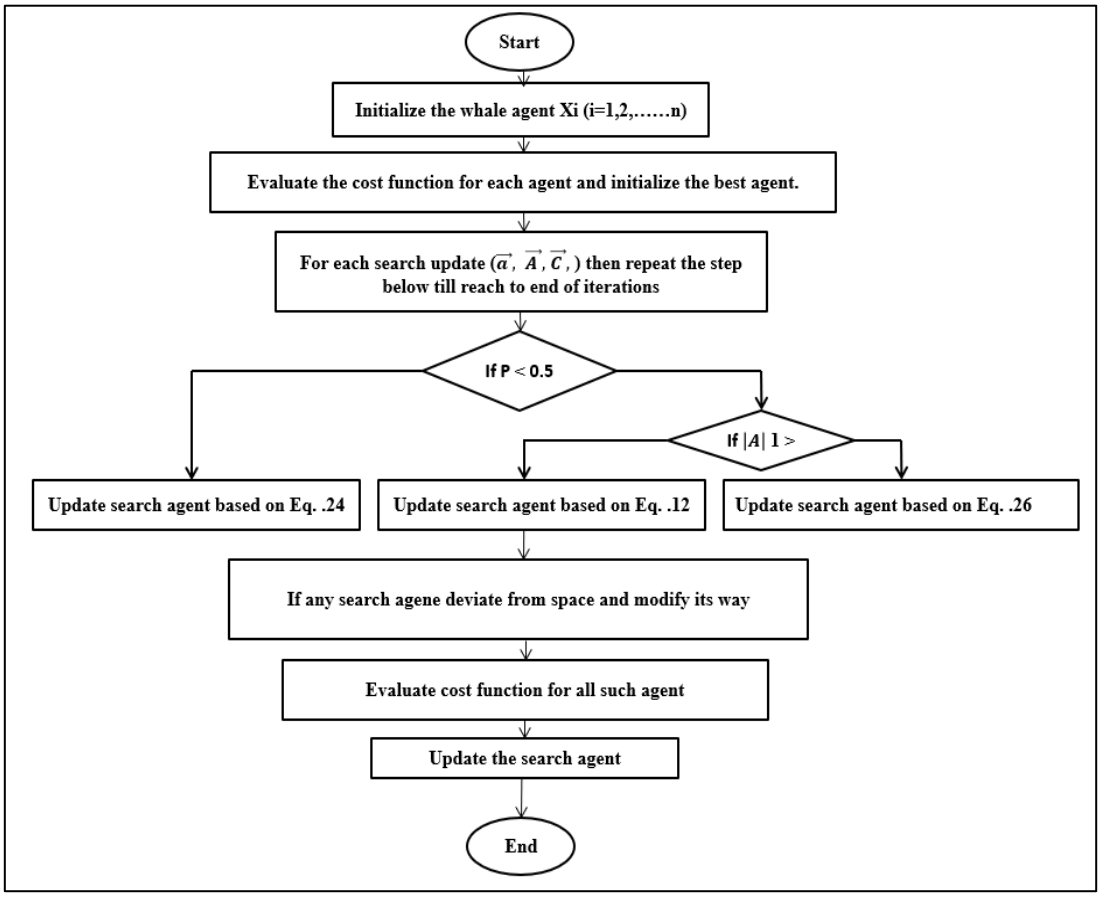


**Figure 3.** Flow Chart of Whale Optimization Algorithm [43].

## 5. RESULT

In MATLAB/Simulink, the Automatic Voltage Regulation (AVR) system of the Iraqi Hamrin Hydroelectric Power Plant is modeled with a PID controller, as shown in Figure 4. The terminal voltage response is recorded during the first 30 seconds. Table 2 presents the terminal voltage characteristics, including maximum deviation, peak time, settling time, and steady-state error.

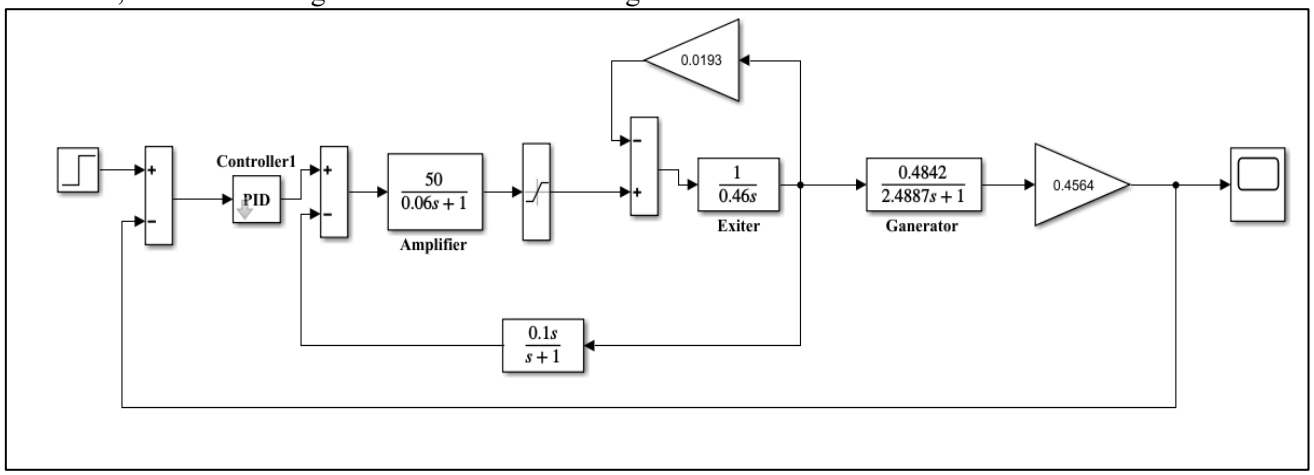


**Figure 4**. MATLAB/Simulink Model of AVR System with a PID Controller

**Table 2.** Terminal Voltage Characteristics without PID

| Variable Without PID | |
|---|---|
| Max. deviation (p.u) | 1.58 |
| Peak time (sec.) | 6.5 |
| Settling time (sec.) | 18 |
| Steady-state error (p.u) | 0.04 |

The modeling in this work was implemented for a real AVR system used in the Hamrin hydroelectric power station. For the original system without PID, the maximum deviation
was 1.58 p.u., the peak time was 6.5 seconds, the settling time was 18 seconds, and the steady-state error was 0.04. These results serve as the standard for comparison with the proposed methods.
To improve the synchronous generator's performance, the PID controller parameters Kp, Ki, and $K_d$ are adjusted through the AVR system to enhance stability and control. The ITAE performance index, which sums the absolute values of cumulative errors, is used to determine optimal controller gains Figure 5.

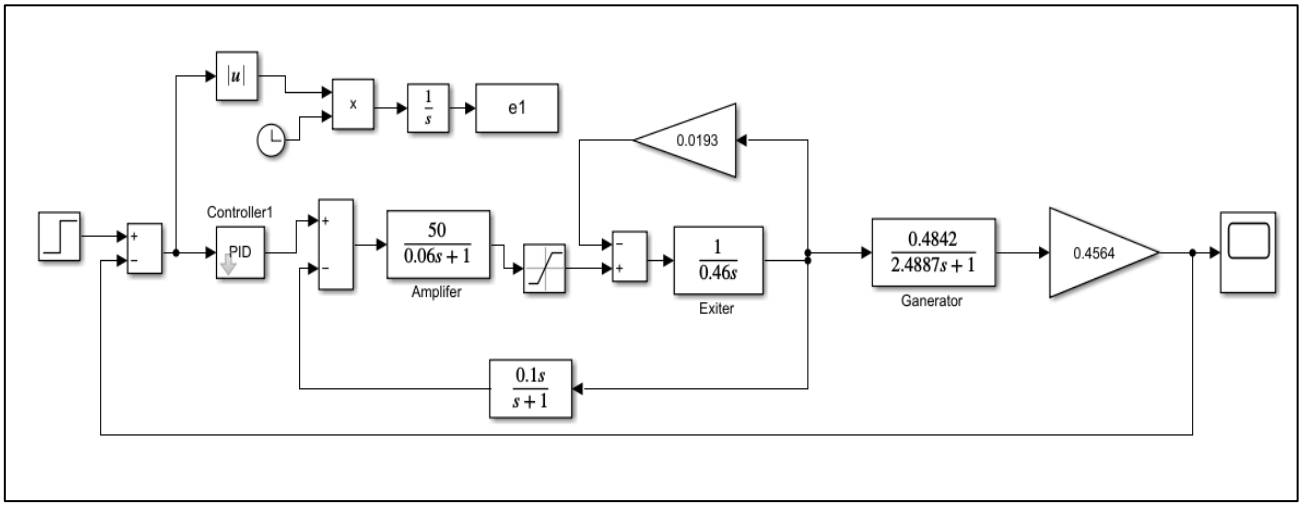


**Figure 5**. Block Diagram of the ITAE-index of the AVR System Model using MATLAB/Simulink

Similarly, the ITSE performance index, which sums the squared cumulative errors, is employed as a cost function to find typical PID settings (Figure 6).

Optimization techniques, including GWO-ITAE, GWO-ITSE, WOA-ITAE, and WOA-ITSE, are applied to minimize persistent errors and achieve an ideal system response.

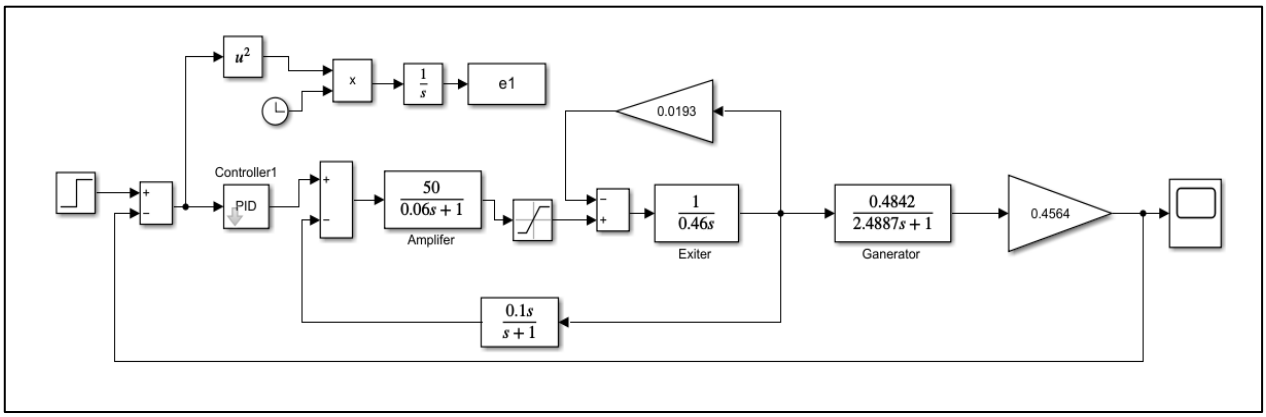


**Figure 6.** Block Diagram of the ITSE-index of the AVR System Model using MATLAB/Simuli

The terminal voltage responses obtained using Gray Wolf Optimization (GWO) and Whale Optimization Algorithm (WOA), including GWO-ITAE, GWO-ITSE, WOA-ITAE, and WOA-ITSE, are shown in Figure 7. Optimal PID is shown in Table 3.
This method preserved a maximum deviation close to 1.06 p.u., while the smallest deviation was achieved with WOA-ITSE (1.03), indicating good voltage stability. The WOA-ITAE method achieved the lowest peak time (5.4 sec), showing a faster response. Peak time (5.8 sec) and settling time (10 sec) of GWO-ITSE indicate a slower but possibly smoother response. GWO-ITAE and WOA-ITSE provided a good balance (peak time less than 6 seconds and settling time less than 8 seconds). All algorithms successfully converged to the same settling point, with a final error of 0.024 p.u.

Comparison between two optimization methods at the same index is GWO-ITAE vs WOA-ITAE: Max deviation of GWO-ITAE (1.05 p.u.) is 0.94% better than WOA-ITAE (1.06), peak time is 5.7 sec (5.56% slower than WOA-ITAE), settling time is 7.8 sec (2.5% faster than WOA-ITAE), and steady-state error is equal (0.024 p.u).GWO-ITSE vs WOA-ITSE: Max deviation of GWO-ITSE (1.03 p.u.) is 0.96% better than WOA-ITSE (1.04), peak time is 5.8 sec (same as WOA-ITSE), settling time is 10.0 sec (33.33% slower than WOA-ITSE), and steady-state error is equal (0.024 p.u). Figure 8 shows comparisons of different optimization methods across performance indicators, presenting enhancements over the base system.

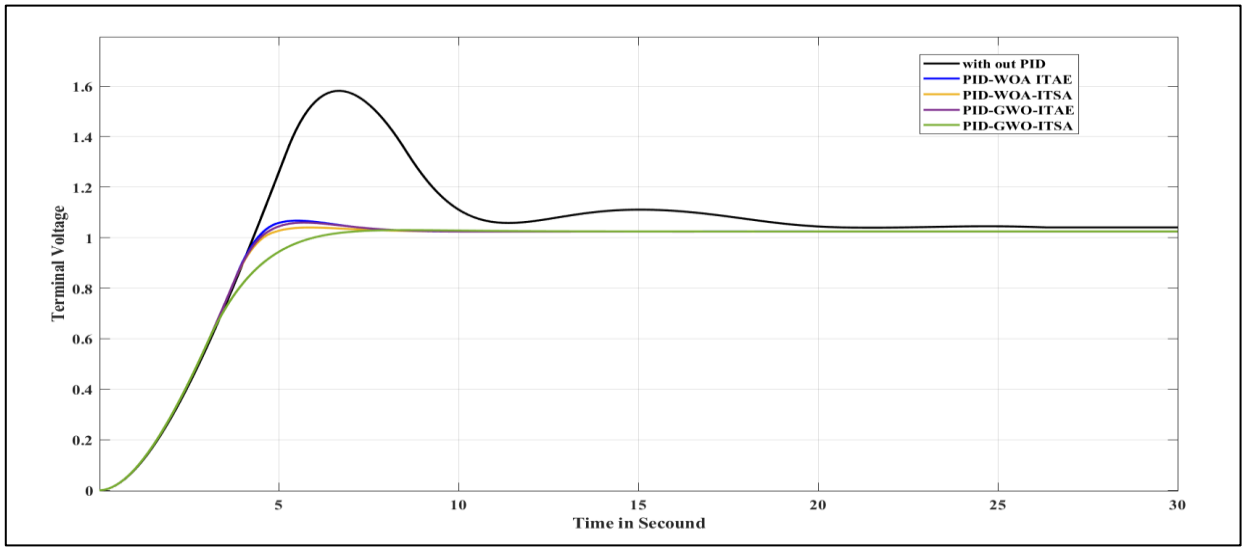


**Figure 7.** Terminal Voltage using Different PID Controllers Optimized by GWO and WOA Algorithms

**Table 3**. Final Optimized PID Controller Gains from Each Tuning Method

| Method | Kp | Ki | Kd |
|---|---|---|---|
| GWO-ITAE | 1.654 | 0.079 | 1.731 |
| GWO-ITSE | 2.000 | 0.065 | 1.669 |
| WOA-ITAE | 2.019 | 0.076 | 1.740 |
| WOA-ITSE | 1.998 | 0.080 | 1.557 |

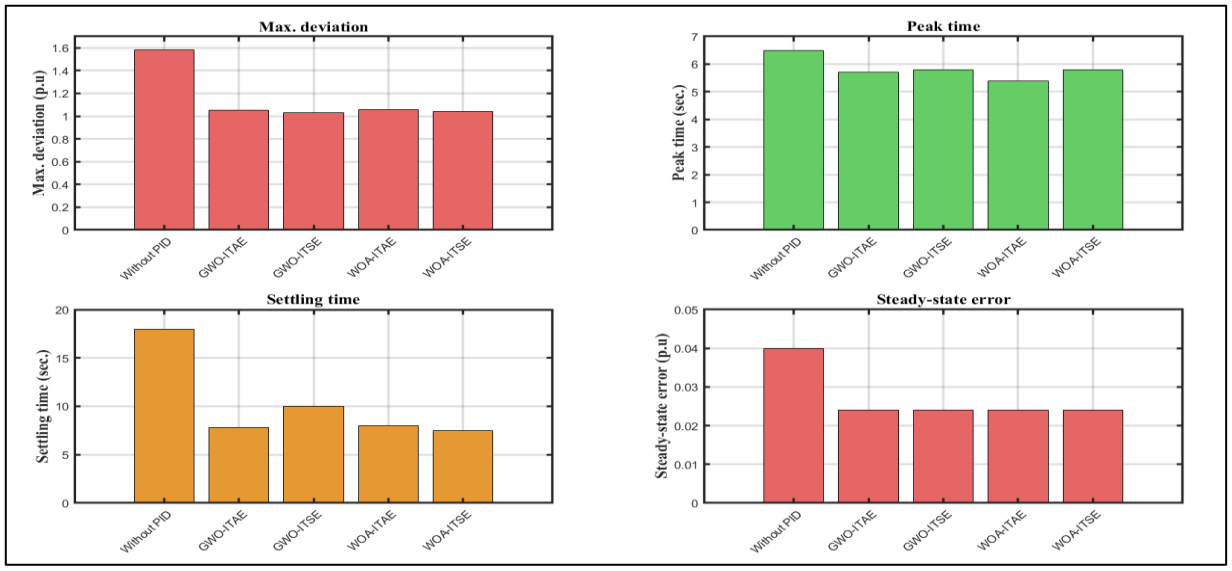


**Figure 8**. Comparison of GWO and WOA Optimization Methods Across ITSE and ITAE Indicators.

The convergence curves of the ITAE and ITSE indices using GWO and WOA are shown in Figures 9 and 10. The results indicate that

The GWO-based PID controller exhibits better convergence and performance compared to the WOA-based PID controller.

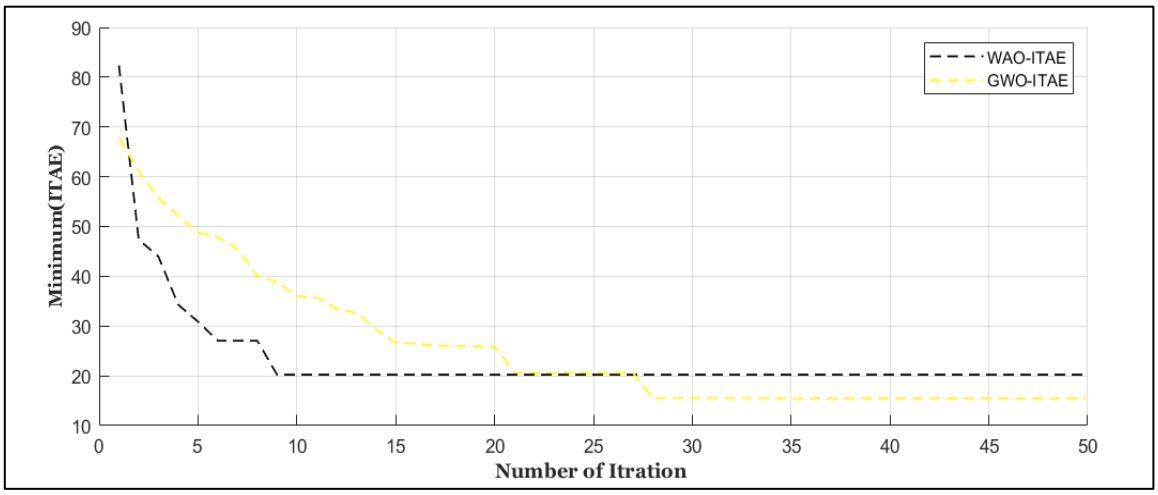


**Figure 9**. Convergence Curve between WOA- ITAE and GWO-ITAE Algorithms

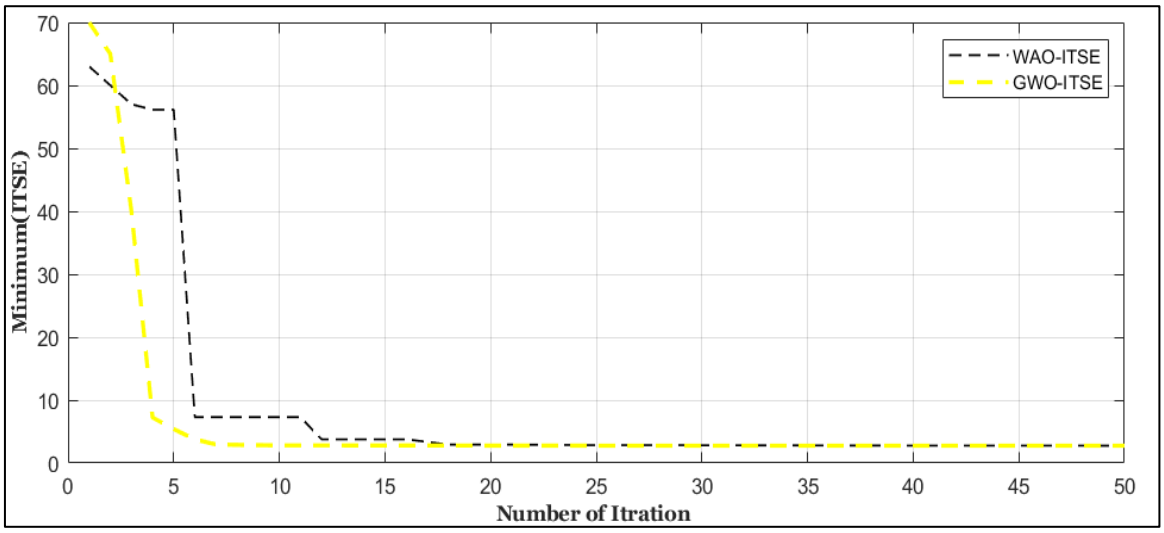


**Figure 10**. The Convergence between the WOA-ITSE and GWO-ITSE Algorithms

To evaluate the performance of the GWO and WOA algorithms, 30 experiments were conducted for each algorithm on the ITSE and ITAE indices. The results showed that the GWO algorithm outperformed the ITSE metric, with a mean value of 10.833 compared to 16.53 for the WOA algorithm. The best value was 8.673 versus 13.221, and the worst value was 13.654 versus 22.110. The standard deviation was 1.621, compared to 2.113, demonstrating the Grey Wolf algorithm's stable performance on this indicator.

The results showed that the GWO algorithm slightly outperformed the Whale algorithm, according to the ITAE index results, with an average value of 14.767 compared to 15.355, respectively. The best values recorded during the experiments were 10 for both algorithms. The worst results recorded over 30 experiments were 18.098 for the Wolf method and 19.238 for the Whale method. The standard deviation recorded for the GWO algorithm was 2.044 compared to 2.346 for the AWO algorithm. In general, we conclude that the Whale algorithm was characterized by more stable performance and less dispersion, compared to some individual good results for the Whale algorithm.

Figure 11 shows a box plot of the two proposed algorithms, along with the performance indices ITSE and ITAE. The figure shows that the GWO algorithm has lower average values than the WOA algorithm. The data dispersion is narrower in the GWO case, which explains the greater stability in performance and lower variance between experimental results. In contrast, the WOA algorithm exhibits greater variation and dispersion in results, although some experiments had good values. Therefore, we conclude that the GWO algorithm has better accuracy and consistency across both indices than the WOA algorithm.

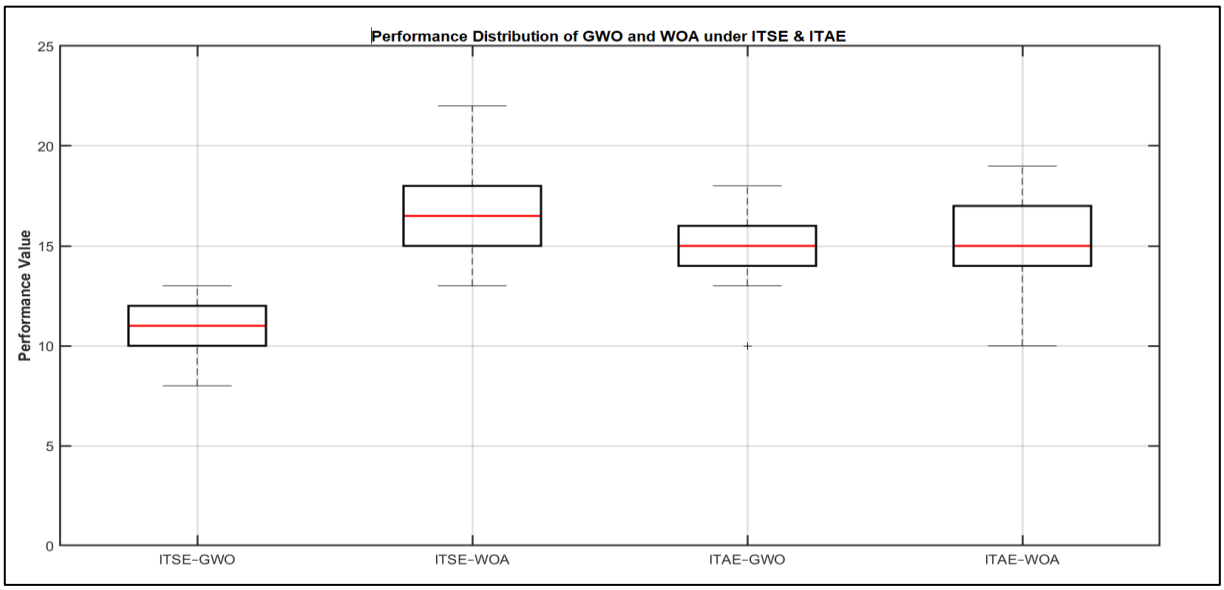


**Figure 11.** Boxplot Comparison of GWO and WOA Algorithms under ITSE and ITAE Performance Indices

## 6. CONCLUSIONS

The goal of this work is to find the best values for the PID controllers in the automatic voltage regulator system at the Hamrin Hydropower Plant. The results without PID showed a maximum voltage deviation of 1.58 p.u., settling time of 18 seconds, and a steady-state error of 0.04. This makes the system unsafe and unstable for practical use.

The results showed a significant improvement when using optimization algorithms to identify PID controllers. The proposed methods (GWO-ITAE, GWO-ITSE, WOA-ITAE, and WOA-ITSE) improved the results and reduced the steady-state error to 0.024 V. WOA-ITAE achieved a peak time of 5.4 s, while WOA-ITSE recorded a maximum deviation of 1.03 V, demonstrating better stability. GWO-ITSE had a slower response (10 seconds settling time) and flexible and suitable voltage changes. GWO-ITAE achieved good and stable performance with acceptable peak time and stability.

When applying proposed algorithms to the two indices, limited differences were found between the results. When using the GWO algorithm on the ITAE indices, the peak was slightly slower than the WOA algorithm. When applying the ITSE indices, the results of the two algorithms were nearly identical, with the WOA algorithm responding faster, while the GWO algorithm was more effective at smooth convergence.

From the PID parameter results recorded using the WOA and GWO algorithms according to the two indicators used, it is clear that the WOA algorithm achieves higher derivative and relative gains, which is why the system response is faster. The GWO algorithm, on the other hand, achieved balanced gains and stable performance, albeit at a slower pace. From the convergence curves of each algorithm, we concluded that the search behavior of each of them differs. The WOA algorithm tends to focus on promising regions within the permitted search range, which increases sensitivity and results stabilize quickly. The GWO algorithm, on the other hand, balances local and global exploration, achieving greater convergence and reliability. This explains the reason for the rapid responses of the Whale algorithm and the guarantee of continuity and robustness of the Grey Wolves algorithm.

Additional experiments were conducted for the two proposed algorithms by increasing the population sizes to 50 and two sets of iterations (200 and 500) to verify the robustness of the results. The results showed that the ITAE and ITSE values for the two optimization algorithms were consistent with the values calculated using a population size of 30 and iterations of 50, with a significant increase in time. For the GWO algorithms, the time increased from 55 seconds (30, 50) to 520 seconds (50, 200) and 1146 seconds (50, 500). For the WOA algorithms, the time increased from 68 seconds (30, 50) to 650 seconds (50, 200) and 1165 seconds (50, 500). The results confirm that the main settings used for the proposed algorithms achieve a balance between computational cost and accuracy.

In general, the choice between the results obtained from both algorithms depends on operational requirements. When a fast system response is required, we use WOA-ITAE, while if stability and robustness are the most important requirements, as is the case for hydropower plants with high inertia, GWO-ITAE is more appropriate.

## References

[1] S. Chatterjee and V. Mukherjee, "PID controller for automatic voltage regulator using teaching-learning based optimization technique," *International Journal of Electrical Power & Energy Systems,* vol. 77, pp. 418-429, 2016. [Online]. Available: https://doi.org/10.1016/j.ijepes.2015.11.010

[2] R. Mok and M. A. Ahmad, "Fast and optimal tuning of fractional order PID controller for AVR system based on

memorizable-smoothed functional algorithm," *Eng. Sci. Technol., Int. J.*, vol. 35, p. 101264, 2022. DOI: 10.1016/j.jestch.2022.101264.

[3] G. A. Salman, A. S. Jafar, and A. I. Ismael, "Application of artificial intelligence techniques for LFC and AVR systems using PID controller," *Int. J. Power Electron. Drive Syst.*, vol. 10, no. 3, pp. 1694–1704, Sep. 2019.

[4] B A. O. Badr et al., "Seamless transition and fault-ride-through by using a fuzzy EO PID controller in AVR system," *Energies*, vol. 15, no. 22, p. 8475, Nov. 2022. DOI: 10.3390/en15228475.

[5] G. Chadar, S. K. Mohaney, and P. Lakra, "Improvement in voltage profile of synchronous generator using PID controller and artificial neural network in automatic voltage regulator," in *2022 IEEE 11th International Conference on Communication Systems and Network Technologies (CSNT)*, Indore, India, Apr. 23-24, 2022, pp. 1-6. DOI: 10.1109/CSNT54456.2022.9787640.

[6] N. Z. Goswami et al., "Performance analysis of the AVR using an artificial neural network and genetic algorithm optimization technique," in *2023 3rd International Conference on Robotics, Electrical and Signal Processing Techniques (ICREST)*, Dhaka, Bangladesh, Jan. 4-6, 2023. DOI: 10.1109/ICREST57604.2023.10070230.

[7] F. Olivas, L. Amador-Angulo, J. Perez, C. Caraveo, F. Valdez, and O. Castillo, "Comparative study of type-2 fuzzy particle swarm, bee colony and bat algorithms in optimization of fuzzy controllers," *Algorithms*, vol. 10, no. 3, p. 101, 2017. DOI: 10.3390/a10030101.

[8] B. T. Chiranjeevi and S. Babu, "Implementation of fractional order PID controller for an AVR system using GA and ACO optimization techniques," *IFAC-PapersOnLine*, vol. 49, no. 1, pp. 456-461, 2016. DOI: 10.1016/j.ifacol.2016.03.096.

[9] B. Ozgenc, M. S. Ayas, and I. H. Altas, "A hybrid optimization approach to design optimally tuned PID controller for an AVR system," in *2020 International Congress on Human-Computer Interaction, Optimization and Robotic Applications (HORA)*, Ankara, Turkey, Jun. 4-6, 2020, pp. 1-6. DOI: 10.1109/HORA49412.2020.9152915.

[10] Z. Bingul and O. Karahan, "Comparison of PID and FOPID controllers tuned by PSO and ABC algorithms for unstable and integrating systems with time delay," *Optimal Control Appl. Methods*, vol. 39, no. 4, pp. 1431–1450, Jul./Aug. 2018. DOI: 10.1002/oca.2408.

[11] A. Mishra, N. Singh, and S. Yadav, "Design of optimal PID controller for varied system using teaching-learning-based optimization," in *Advances in Computing and Intelligent Systems* (Lecture Notes in Networks and Systems, vol. 108), Singapore: Springer, 2020, pp. 153-163. DOI: 10.1007/978-981-15-0222-4_14.

[12] H. M. Hasanien, "Design optimization of PID controller in automatic voltage regulator system using Taguchi combined genetic algorithm method," *IEEE Syst. J.*, vol. 7, no. 4, pp. 825–831, Dec. 2013. DOI: 10.1109/JSYST.2012.2225732.

[13] H. Shayeghi and J. Dadashpour, "Anarchic society optimization based PID control of an automatic voltage regulator (AVR) system," *Electr. Electron. Eng.*, vol. 2, no. 4, pp. 199–207, 2012.

[14] S. Anbarasi and S. Muralidharan, "Enhancing the transient performances and stability of AVR system with BFOA tuned PID controller," *J. Control Eng. Appl. Inform.*, vol. 18, no. 1, pp. 20–29, Mar. 2016.

[15] S. Vivekanandan et al., "Chaotic differential evolution algorithm-based PID controller for automatic voltage regulator system," *Int. J. Sci. Res. Publ.*, vol. 5, no. 6, pp. 431–436, Jun. 2015.

[16] E. Çelik, "Incorporation of stochastic fractal search algorithm into efficient design of PID controller for an automatic voltage regulator system," *Neural Comput. Appl.*, vol. 30, no. 6, pp. 1991–2002, Jun. 2018. DOI: 10.1007/s00521-017-2943-6.

[17] M. H. Suid and M. A. Ahmad, "Optimal tuning of sigmoid PID controller using Nonlinear Sine Cosine Algorithm for the Automatic Voltage Regulator system," *ISA Trans.*, vol. 128, pp. 265–286, Sep. 2022. DOI: 10.1016/j.isatra.2022.01.014.

[18] P. Sirsode, A. Tare, and V. Pande, "Design of robust optimal fractional-order PID controller using Salp Swarm Algorithm for Automatic Voltage Regulator (AVR) system," in *2019 Sixth Indian Control Conference (ICC)*, Hyderabad, India, Dec. 18-20, 2019, pp. 415-420. DOI: 10.1109/INDIANCC.2019.8715604.

[19] N. Razmjooy, M. Khalilpour, and M. Ramezani, "A new meta-heuristic optimization algorithm inspired by FIFA World Cup competitions: theory and its application in PID designing for AVR system," *J. Control Autom. Electr. Syst.*, vol. 27, no. 4, pp. 419–440, Aug. 2016. DOI: 10.1007/s40313-016-0242-6.

[20] D. K. Sambariya and T. Gupta, "Optimal design of PID controller for an AVR system using monarch butterfly optimization," in *2017 International Conference on Information, Communication, Instrumentation and Control (ICICIC)*, Indore, India, Aug. 17-19, 2017, pp. 1-6. DOI: 10.1109/ICOMICON.2017.8279118.

[21] Bingul, Zafer, and Oguzhan Karahan. "A novel performance criterion approach to optimum design of PID controller using cuckoo search algorithm for AVR system." Journal of the Franklin Institute 355.13 (2018): 5534-5559.

[22] R. Pradhan, S. K. Majhi, and B. B. Pati, "Design of PID controller for automatic voltage regulator system using Ant Lion Optimizer," *World J. Eng.*, vol. 15, no. 3, pp. 373-387, Jun. 2018. DOI: 10.1108/WJE-09-2017-0295.

[23] E. Köse, "Optimal control of AVR system with tree seed algorithm-based PID controller," *IEEE Access*, vol. 8, pp. 89457–89467, 2020. DOI: 10.1109/ACCESS.2020.2993756.

[24] S. Ekinci and B. Hekimoğlu, "Improved kidney-inspired algorithm approach for tuning of PID controller in AVR system," *IEEE Access*, vol. 7, pp. 39935–39947, 2019. DOI: 10.1109/ACCESS.2019.2906980.

[25] S. A. N. Burnaz and M. Ş. Ayas, "Effects of objective function in PID controller design for an AVR system," *Int. J. Appl. Math. Electron. Comput.*, vol. 8, no. 4, pp. 245–255, Dec. 2020. DOI: 10.18100/ijamec.801466.

[26] G. A. Salman, H. I. Hussein, and M. S. Hasan, "Enhancement the dynamic stability of the Iraq's power station using PID controller optimized by FA and PSO based on different objective functions," *Elektroteh. Vestn.*, vol. 85, no. 1/2, pp. 42–48, 2018. http://ev.fe.uni-lj.si/1-2-2018/Salman.pdf

[27] A. H. Ibrahim et al., "Design and implementation of fuzzy logic-based AVR system using Arduino," *IEEE Access*, vol. 10, pp. 24374–24385, 2022. DOI: 10.1109/ACCESS.2022.3155361.

[28] M. H. Abbas and S. H. Al-Dabbagh, "Fuzzy logic controller based AVR for enhancing voltage stability," *Iraqi J. Electr. Electron. Eng.*, vol. 16, no. 1, pp. 12–18, Jun. 2020. http://ijeee.edu.iq/index.php/ijeee/article/view/246.

[29] A. F. M. Saifuddin and A. A. El-Samahy, "SMC-based AVR control scheme for synchronous generator using reduced order model," *IEEE Access*, vol. 9, pp. 88540-88549, 2021. DOI: 10.1109/ACCESS.2021.3089039.

[30] T. S. Ahmad et al., "Design of AVR using sliding mode controller in presence of disturbances," *Indones. J. Electr. Eng. Comput. Sci.*, vol. 21, no. 2, pp. 1002–1010, Feb. 2021. DOI: 10.11591/ijeecs.v21.i2.pp1002-1010.

[31] T. Patnaik and B. Subudhi, "Neural network-based adaptive AVR system," *J. Control Autom. Electr. Syst.*, vol. 31, no. 4, pp. 843–857, Aug. 2020. DOI: 10.1007/s40313-020-00593-w.

[32] M. M. Abdelkarim and M. E. Ammar, "A deep learning based AVR for uncertain systems," *J. Electr. Syst. Inf. Technol.*, vol. 8, no. 2, pp. 450–460, Dec. 2021. DOI: 10.1186/s43067-021-00042-x.

[33] R. R. Rego and A. K. Sinha, "Optimal AVR design using LQR and genetic tuning," *Electr. Power Compon. Syst.*, vol. 48, no.

3-4, pp. 312–323, Mar. 2020. DOI: 10.1080/15325008.2020.1758853.

[34] M. Azazi et al., "LQR based AVR design enhanced by grey wolf optimization," *Int. J. Electr. Power Energy Syst.*, vol. 118, Art. no. 105789, Jun. 2020. DOI: 10.1016/j.ijepes.2020.105789.

[35] R. Sharma and P. S. Bhowmik, "Adaptive model predictive control based AVR for uncertain loads," *Electr. Power Syst. Res.*, vol. 187, Art. no. 106487, Oct. 2020. DOI: 10.1016/j.epsr.2020.106487.

[36] C. Muro, R. Escobedo, L. Spector, and R. Coppinger, "Wolf-pack (Canis lupus) hunting strategies emerge from simple rules in computational simulations," *Behav. Processes*, vol. 88, no. 3, pp. 192–197, Nov. 2011. DOI: 10.1016/j.beproc.2011.09.006.

[37] D. Jitkongchuen, "A hybrid differential evolution with grey wolf optimizer for continuous global optimization," in *Proc. 2015 7th Int. Conf. Inf. Technol. Electr. Eng. (ICITEE)*, Chiang Mai, Thailand, Oct. 29-30, 2015, pp. 51–54. DOI: 10.1109/ICITEED.2015.7408878.

[38] K. Jaiswal, H. Mittal, and S. Kukreja, "Randomized Grey Wolf optimizer (RGWO) with randomly weighted coefficients," in 2017 10th Int. Conf. Contemp. Comput. (IC3), Noida, India, Aug. 10-12, 2017, pp. 1–3, 2018. DOI: 10.1109/IC3.2017.8284344.

[39] B. M. Hussein, A. I. Jaber, M. W. Abdulwahhab, H. J. Mohammed, and N. V. Korovkin, "Application of Intelligent Optimization Algorithms on Economic Dispatch Problem," in Proc. 2024 XXVII Int. Conf. Soft Comput. Meas. (SCM), May 2024, pp. 453–456.

[40] S. Mirjalili and A. Lewis, "The whale optimization algorithm," *Adv. Eng. Softw.*, vol. 95, pp. 51–67, May 2016. DOI: 10.1016/j.advengsoft.2016.01.008.

[41] J. Zhang et al., "Parameter optimization of PID controller based on an enhanced whale optimization algorithm for AVR system," Oper. Res., vol. 23, no. 3, Art. no. 44, Jul. 2023. DOI: 10.1007/s12351-023-00784-8.

[42] K. Simhadri et al., "Frequency and voltage control of multi-area multisource power system using whale optimization algorithm," in *Proc. XVIII Int. Conf. Data Sci. Intell. Anal. Inf.* (Lecture Notes in Networks and Systems, vol. 725), Cham, Switzerland: Springer, 2023. DOI: 10.1007/978-3-031-36698-2_31

[43] L. H. Abood and B. K. Oleiwi, "Design of fractional order PID controller for AVR system using whale optimization algorithm," *Indones. J. Electr. Eng. Comput. Sci.*, vol. 23, no. 3, pp. 1410–1418, Sep. 2021